6

PET-MMT and PET-PEN-MMT Nanocomposites by Melt Extrusion

Fausto Calderas, Guadalupe Sánchez-Olivares[1], Edtson Emilio Herrera-Valencia, Antonio Sánchez-Solís and Octavio Manero
Universidad Nacional Autónoma de México,
Instituto de Investigación en Materiales,
[1]CIATEC, A.C.
México

1. Introduction

Polymer nanocomposites have attracted a great deal of interest in the scientific and industrial fields because of remarkable improvements achieved in the physical and mechanical properties at very low filler loadings. For example, the diffusion of gas molecules is largely retarded by the presence of randomly oriented clay particles.

These new class of materials can be obtained by means of two main processes: in-situ polymerization of monomers in the presence of nanoparticles and the use of polymer processing techniques such as extrusion [Okamoto, M. 2006 and Suprakas, S. R. 2003]. The use of clay particles to produce nanocomposites is a usual practice; however, clay has to be usually organically modified to induce affinity with the polymer matrix [Kráčalík, M. et al 2007; Vidotti, S. E. et al 2007]. The improvement of nanocomposite properties depends on different factors, for example, a good dispersion of clay particles in nano-scale within the polymer matrix. The nanocomposites obtained by melt extrusion require initially, an intercalation process of the polymer macromolecule into the clay galleries and finally clay exfoliation in the polymer matrix. This process is diffusion-controlled and requires long residence times under the pressure buildup produced inside the extruder. However, high residence times or high screw speeds may conduce to polymer degradation. Therefore, optimum process conditions need to be investigated in order to produce high performance nanocomposites.

Moreover, it has been found that clay exfoliation may not be a sufficient condition to obtain optimum properties; clay platelets dispersion and polymer-clay interaction are also key features to consider.

In this chapter, poly(ethylene terephthalate)-montmorillonite clay (PET-MMT) and poly(ethylene terephthalate)-poly(ethylene naphthalene 2,6-dicarboxylate)-montmorillonite clay (PET-PEN-MMT) nanocomposites were prepared and characterized. Maleic anhydride (MAH) is used as the compatibilizing agent in the blend and its effect is also studied. In both nanocomposite blends, optimum processing conditions were investigated to achieve improved tensile properties. The preparation of the PET-PEN polymer matrix also requires special care since a transesterification reaction between these two polymers is induced by

the process; the transesterification (NET) reaction between PET and PEN is affected by temperature and residence time in the extruder; nevertheless the presence of clay particles was also found to affect this reaction. Regarding thermal properties, crystallization enthalpy was found to diminish in the clay presence, i.e. the clay restricts the crystallization of the polymer matrix. Finally, the rheological behavior of these materials is still far from being fully understood. An increase in the steady shear flow viscosity with the clay content has been observed for most systems while in some cases the viscosity decreases with low clay loading. Other important characteristic of exfoliated nanocomposites is the loss of the complex viscosity Newtonian plateau in oscillatory shear flow. Transient rheology experiments have also been used to study the rheological response of polymer nanocomposites. The degree of exfoliation is associated to the amplitude of stress overshoots in start-up experiments. Two main modes of relaxation have been observed in the stress relaxation (step shear) test, namely, a fast mode associated to the polymer matrix and a slow mode associated to the polymer-clay network. Rheology results are discussed and instantaneous stress relaxation curves are presented for the PEN, PEN-PET and PET-PEN-MMT systems. A Fourier Transform (FT) frequency response was obtained from the relaxation curves and compared to the linear oscillatory data, which leads to an extended frequency region. The results were modeled by a rheological equation of state which accounts for the structure formation-destruction dynamics during flow; this equation is presented in the theoretical section in full detail. Relaxation time spectra are presented and compared for both rheological tests, namely, instantaneous stress relaxation and linear oscillatory flow. Additional studies using scanning electron microscopy (SEM) are presented, which reveal the presence of a slip layer in capillary flow for nanocomposite as opposed to the unfilled system which may explain the viscosity decrease observed in these systems.

Still further investigation is required to assess the main reinforcement mechanism of the nanoparticles, since it is not clearly resolved whether exfoliation or good dispersion are required.

2. PET-PEN Transesterification reaction

The transesterification reaction that occurs between poly(ethylene terephthalate) and poly(ethylene 2,6-naphthalene dicarboxylate), PET and PEN respectively, can be represented by the following equation.

$$TET + NEN \underset{\vec{k}}{\overset{k'}{\rightleftharpoons}} 2TEN \tag{1}$$

where: TET= terephthalate–ethylene–terephthalate, NEN= terephthalate–ethylene–naphthalene and TEN= terephthalate–ethylene–naphthalene. The equilibrium constant for this reaction can be expressed as:

$$K'' = \frac{K}{K'} = \frac{\left[\mathrm{TEN}_{eq}\right]^2}{\left[\mathrm{TET}_{eq}\right]\left[\mathrm{NEN}_{eq}\right]} \tag{2}$$

where subscript "eq" refers to equilibrium reaction conditions.

Several authors have given attention to the kinetics of thistransesterification reaction describing it as a second order reversible reaction [Chen et al. 1996, Lee et al, 1999, Alexandrova et al. 2000].
However, the equilibrium constant was considered in those works as equal to one, which presumes that the reaction of equimolar amounts of thereactants leads to equal concentrations of molar fractions of the species when the transesterification reaction reaches equilibrium.
Based on the results above mentioned, the mechanism and kinetics of the transesterification reaction in poly(ethylene terephthalate) and poly(ethylene 2,6-naphthalene dicarboxylate) polymer blends was simulated using model compounds of ethylenedibenzoate (BEB) and ethylene dinaphthoate (NEN)[Alexandrova et al. 2000]. An additional investigation dealt with the actual melt extrusion of the blend below the critical reaction temperature in the extruder [Medina et al. 2004]
Prior to melt compounding in the extruder, the PET and PEN polymers were previously dried in a Cole–Palmer vacuum oven at 120 °C with-45mm Hg pressure during 10 h. Extrusion was carried out in a Haake-Rheocord 90 TW-100 twin-screw conical counter-rotating extruder of 331 mm length, with temperature profile of 230, 240 and 250 °C and screw speed of 30RPM. The resulting mixture was milled and placed in open glass ampoules, 2 g each. Sets of eight samples were immersed into a thermo-stated silicon oil bath at 300 and 320°C during defined time intervals. Thereafter, samples were cooled to room temperature. Solids obtained were dissolved in a 70/30 vol. $CDCl_3$ and CF_3COOD solvent mixture for ^1H NMR analyses. NMR spectra were obtained in a BruckerAdvance 400 spectrometer.
The formation of the TEN copolyester is depicted in figure 1. The transesterification kinetics was followed by measuring the integral intensities of the aliphatic proton signals for TET, NEN and TEN. As the reaction progresses, a copolyester is formed and this is evidenced as an intermediate signal (TEN) between those corresponding to TET and NEN. Values for the equilibrium constant were found to lie between 3.8-4, from which authors determined that the value of the equilibrium constant was four:

$$K'' = 4K' \tag{3}$$

It was also confirmed that heating the blend above 300 °C direct ester–ester exchange mechanism produces the TEN sequences with reversible second order kinetics. The reaction order was confirmed using pseudofirst order conditions with a 10-fold excess of either PET or PEN. Kinetics was followed by the limiting reactant disappearance, as well as the formation of the TEN product. Kinetic data obtained were treated in terms of first order kinetics, according to the following equation:

$$\ln \frac{[\mathrm{NEN}]_0}{[\mathrm{NEN}]} = \bar{k}t \tag{4}$$

A linear tendency of concentrations ratio versus time was obtained (not shown) for the PET/PEN blend with 10:1 mole ratio, indicating that the transesterification reaction in PET/PEN system is first order regarding either of the reagents (Same results were found when PEN was in excess). Thus it was concluded that the overall order of the reaction is second order.

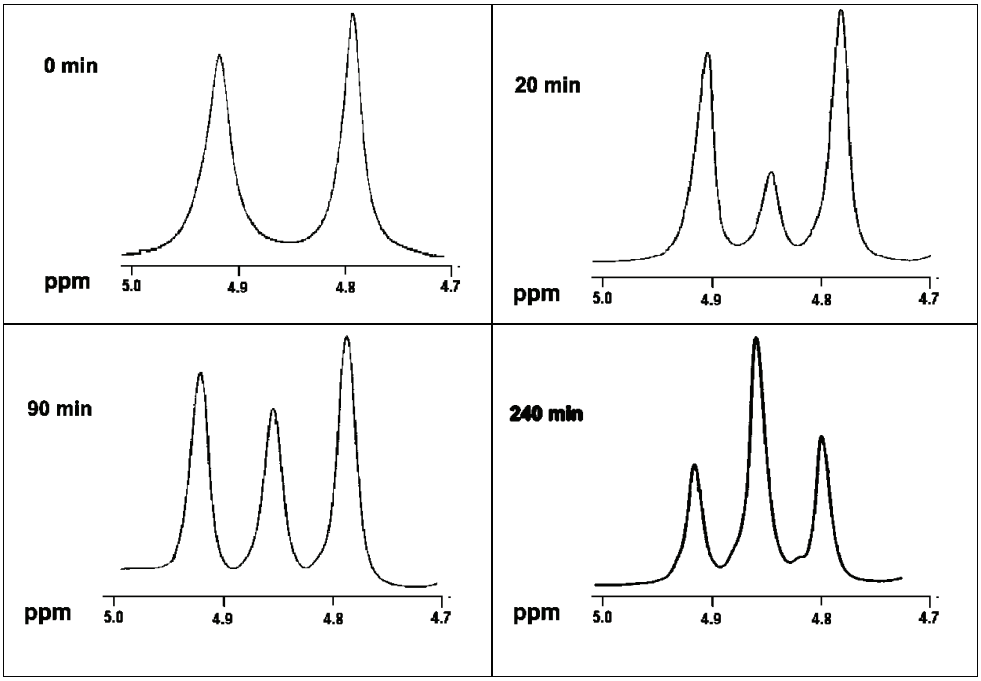

Fig. 1. Proton MRN spectra of the formation of the TEN copolyester in the TET/NEN blend at different stages of the transesterification reaction

The influence of extrusion residence time and temperature on the kinetics of the transesterification reaction has been also studied using a 30 mm diameter co-rotating twin-screw extruder (Werner & Pfleiderer ZSK30) with a general-purpose screw configuration including two rows of kneading elements (15 elements by row and 5 mm width each) and L/D = 30 [Sánchez-Solís et al. 2005a]. Three extrusion profile temperatures and two residence times were studied: temperature profile 1 (262-265-269-267-270 °C), temperature profile 2 (230-281-278-282-280°C) and temperature profile 3 (273-291-290-290-290°C). The extent of transesterification, i.e. the percentage of naphthalene-ethylene-terephthalate blocks (NET) as compared to the total terephthalate-ethylene-terephthalate blocks (TET) and naphthalene-ethylene-naphthalene blocks (NEN) was derived by spectral deconvolution of the peaks corresponding to each group (see fig. 1) i.e. peaks at 4.9 ppm NEN, 4.8 ppm TET and 4.85 ppm NET (peak due to transesterification) were measured.

It was found that the kinetics of the transesterification reaction was different in profile 3 as compared to the other two profiles studied. Residence time affected in a negative way the production of NET groups (groups related to transesterification reaction) at profiles 1 and 2, while at profile 3 the effect was the opposite: percentage of NET groups increased with residence time. Finally, profile 3 was reported to produce more random copolymer structures during transesterification reaction, i.e. increasing the degree of transesterification leads to higher proportion of random sequences and thereby reducing blend performance [Chen et al. 1996; Lee et al. 1999], while the other two profiles produced more block copolymers.

Finally, the degree of transesterification has been reported to be reduced in the presence of clay particles [Sánchez-Solís et al. 2005b]. Moreover, the particles need not to be organically modified to cause this effect. The hydrophilic clay is highly incorporated in the polymer and presumably has a low concentration at the surface, as evidenced by contact-angle measurements. Show a predominantly hydrophobic character of the clay surface. This blend also presents a large solid-like behavior, which is further discussed in the rheology section.

3. Preparation of nanocomposites by melt extrusion

3.1 PET nanocomposites

Polymer nanocomposites can be obtained by two general routes: the first one is the polymerization of monomers in contact with the nanoparticles (in situ polymerization), and the second one implies the use of existing processing equipment to melt compound the nanocomposite. An example of the latter is reactive extrusion.

In the extrusion process, the nanocomposites are formed initially by intercalating the polymer chains inside the clay galleries gap; this intercalation is the initial step obtain full exfoliation of the clay. However, a complete intercalation requires low screw speeds with the consequent long average residence times within the extruder. This, however, can lead to polymer degradation. In order to avoid polymer degradation, different screw configurations, chemically modified clays or a combination of both can be used. Furthermore, clay exfoliation may not be a sufficient condition to obtain high performance nanocomposites, other factors like nanoparticle-polymer matrix interaction can be considered.

Production of PET-Montmorillonite clay nanocomposites by extrusion has been reported in the literature [Sánchez-Solís et al. 2003]. Additives such as Maleic Anhydride (MAH) and Pentaerythrytol (PENTA) were used to induce compatibility between hydrophilic clay and hydrophobic polymer matrix. MMT was chemically modified with a quaternarium ammonium salt. A co-rotating twin screw extruder (Werner & Pfleiderer ZSK30) was used to melt compound the nanocomposites. In this study clay concentrations up to 2% were considered because higher concentrations caused a decrease in the glass transition temperature. It was reported that crystallization temperature is reduced as a function of clay content; this effect is even more pronounced when additives are used during melt compounding. On the contrary, when the nanocomposites are produced by in-situ polymerization, clay content was reported to have little effect on the crystallization temperature [Ke et al. 1999]. Additives (MAH and PENTA) were reported to increase the crystallinity of the nanocomposites which resulted in superior mechanical properties [Sánchez-Solís et al. 2003] as will be discussed in the mechanical properties section.

The effect of modifying the MMT clay prior to melt compounding with PET by using additives such as alkylammonium chlorides from amines of various chain lengths as well as MAH and PENTA has also been reported [Sánchez-Solís et al. 2004]. The objective of using the alkylammonium chlorides is to impart the nanoclays with functional groups to enhance the polymer-clay interaction and thus facilitate the production of exfoliated and dispersed polymer nanocomposite systems. A Haake Rheocord 90 TW-IOO twin-screw conical counter-rotating extruder of 331 mm length was used for blending. Properties for these nanocomposites will be discussed in the following sections (4-6).

3.2 PET-PEN nanocomposites

The production of PET-PEN-montmorillonite clay nanocmposite blends by extrusion has been reported previously [Sánchez-Solís et al. 2005b]. A quaternary alkylammonium compound (octadecylammoniumchloride) and maleic anhydride were used to modify the surface properties of sodium montmorillonite clay particles. After this process, the particles were mixed with poly(ethylene terephthalate) (PET) and poly(ethylene naphthalene 2,6 dicarboxylate) (PEN) to produce blends whose properties were examined in detail. Blends were prepared in a Leistritz LSM34 corotating twin-screw extruder (Leistritz, Nuremberg, Germany) equipped with a volumetric feeder working under a nitrogen atmosphere to prevent moisture absorption and consequent hydrolysis or chemical degradation of the polyesters.

Preparation of the polymer nanocomposites was carried out at 90, 9 and 1 wt% PET, PEN and clay contents, respectively, with 50 rpm extruder screw rotational velocity (corresponding approximately to 2 min residence time). Three clay types were used in the blends: sodium montmorillonite clay (clay–Na+), maleic anhydride-modified clay (clay–MAH) and alkylammonium-modified clay with n-octadecylamineas precursor (clay–C18).

Glass transition temperature (Tg), crystallization temperature (Tc) and melting temperature (Tm) were measured for the three blends (Table 1). While crystallization and melting enthalpies are similar for PET–PEN/clay–Na+and PET–PEN/clay–C18, differences are observed in the clay–MAH blend. The latter has substantially lower enthalpies of crystallization and melting than those of the other systems. The melting enthalpy for this blend is even lower than those of neat polymers. These results indicate that crystallization is largely restricted and proceeds in a very slow manner, which leads to a large proportion of the amorphous phase with high transparency.

Sample	Tg (°C)	Tc (°C)	Δ Hc (J/g)	Tm (°C)	Δ Hm (J/g)
PET	71	-	-	242	40
PEN	116	-	-	258	36
PET-PEN	75	161	18	244	18
PET-PEN/clay-Na+	75	138	198	248	228
PET-PEN/clay-MAH	71	139	21	248	27
PET-PEN/clay-C18	75	143	185	247	216

Table 1. Thermal properties of PET–PEN/clay blends and neat polymers

Another important remark of this study is the fact that from contact angle measurements at the surface of extruded samples reveal that the particle concentration at the surface decreases with respect to that in the bulk, i.e. In spite of the fact that clay–Na+ is hydrophilic, the surfaces of all samples show a hydrophobic character. This will be discussed further in the morphology section.

4. Mechanical properties

4.1 PET-PEN blends

Mechanical properties of bottles made by injection blow molding after melt extrusion have been reported [Sánchez-Solís et al. 2005a]. Sample specimens were obtained from the bottles

in the longitudinal direction. The processing conditions to obtain bottles with high mechanical properties (tensile strength) were 270°C with 4 min processing time and PEN contents of 15-20%. With the maximum tensile strength obtained for the blend containing 15 wt % of PET. Bottles made from this blend had a tensile strength 2.6 times higher than pure PEN and 3.6 times that of pure PET indicating some synergistic mechanism.
Also, Young's modulus attains a maximum (2.3 times that of PET and 1.6 times that of PEN) when the PEN content is 15wt % at the mentioned processing conditions. Mechanical properties showed no direct relation with % transesterification.

4.2 PET-nanocomposites

Mechanical properties of bottles produced from PET-MMT clay nanocomposites have also been reported as mentioned in section 3.1 [Sánchez-Solís et al. 2003]. After melt compounding the nanocomposite, bottles were produced in an injection-stretch blow-molding machine AOKI in one step with a temperature profile of 275 °C at the feeding section and 320 °C at the injection nozzle, with mold temperature of 16 °C. Bottles were reported to be transparent with a slight brown coloring. Specimens for mechanical testing were cut out from bottles in the longitudinal direction. All specimens for testing have the same thermo-mechanical history so as to avoid the effect of sample degradation on mechanical properties. In this study clay particles did not showed complete exfoliation, nevertheless, the use of additives to improve polymer-particle affinity produced nanocomposites with superior mechanical properties. However, in some samples, improved mechanical properties were achieved without compatibility additives: 30% and 32% maximum enhancement in tensile strength and Young´s modulus. These results indicate that an important issue to consider in preparing polymer nanocomposite is particle dispersion, which can be as important as exfoliation and polymer-clay affinity.
The effect of different modified MMT clays on the mechanical properties of PET nanocomposites has been given attention [Sánchez-Solís et al. 2004]. Specimens for mechanical testing were produced by injection. The clay was modified prior to melt compopunding with PET and different additives were used to modify the blend: Maleic Anhydride (MAH), Pentaerythritol (PENTA) and alkylammonium chlorides from amines of various chain lengths such as n-Decacylammonium, n-Dodecylammonium, n-Tetradecylammonium, and n-Octadecylammonium. It was found that the interlayer distance in the clay varied according to the additive used, however this interlayer distance did not show a direct relation to the amine chain length.
Mechanical properties of unmodified and chemically modified nanoparticles (with MAH and PENTA respectively) are discussed first. A direct relation between clay content and Young´s modulus was found for the unmodified and modified clay. The rate of crystallization of the nanocomposites was reported to have a threefold increase as compared to pure PET, indicating that the nanoparticles have a nucleating effect. This increased crystallization affected directly to the mechanical properties producing nanocomposites with higher modulus than that of pure PET, but with reduced strain at break i.e. cristallinity generates more fragile materials. This was the general effect for the nanocomposites with modified clay using only one additive; in fact, PENTA modified clay produced the nanocomposite with highest Young´s modulus and tension strength at 3% and 1% content, respectively. However when MAH modified clay was melt compounded with the polymer and PENTA was added. The resulting nanocomposite showed the highest tensile strength and deformation at break, indicating a synergistic mechanism between MAH and PENTA.

For the case of the amine modified clays, only two systems showed complete exfoliation one of which showed the highest tension strength and deformation at break (1% clay modified with n-Dodecylammonium) indicating that in this case, exfoliation plays a key role in obtaining superior mechanical properties. Molecular weight in all samples was reported to have little or no modification with clay addition.

4.3 PET-PEN nanocomposites

In the case of PET-PEN-MMT nanocomposites, three kinds of clays have been used: unmodified (clay-Na^+), maleic anhydride (clay-MAH) and octadecylammonium chloride (clay-C18) modified clays. The effect of clay modification on the mechanical properties of the extrusion melt compounded nanocomposite has been reported [Sánchez-Solíset et al. 2005b]. A reduction of the tensile strength as compared to pure PET or PEN is reported, while strain at break increases (with respect to the value of pure PEN). The lowest tensile strength and strain at break values were reported for the blend made with clay–C18. This system was not exfoliated and the blend appears more fragile, hence confirming the lower compatibility of the ingredients of this blend when compared to those of the exfoliated clays (see Table 2).

Sample	Tensile strength [Mpa]	Elastic modulus [Mpa]	Strain at break [%]	x-ray data
PET	51	1447	917	-
PEN	70	1752	356	-
PET-PEN	50	1296	525	-
PET-PEN/clay-Na+	42	1369	663	Exfoliated
PET-PEN/clay-MAH	46	1383	756	Exfoliated
PET-PEN/clay-C18	38	1571	19	33.24

Table 2. Tensile Mechanical properties of PET-PEN-MMT nanocomposites and neat polymers

5. Morphology

Although morphology has not been extensively studied in PET-PEN-MMT nanocomposites there are some interesting results in this field, for example, Figure 2, shows three micrographs for pure PET (a), 1% (b) and 2% (c) Dodecylammonium modified clay [Sánchez-Solís et al. 2004]. In (a) PET morphology presents the typical ductile fracture with voids indicating high energy absorption. Sample (b) corresponds to an exfoliated sample (discussed at the end of section 4.2) where ductile fracture with multilayer formation is observed and matrix yielding is present. Sample (c) presents no exfoliation morphology, exhibiting irregularities and fracture occurring at various positions, indicating fragile fracture (as verified by the low strain at break value, 2.6%).

a)

b)

c)

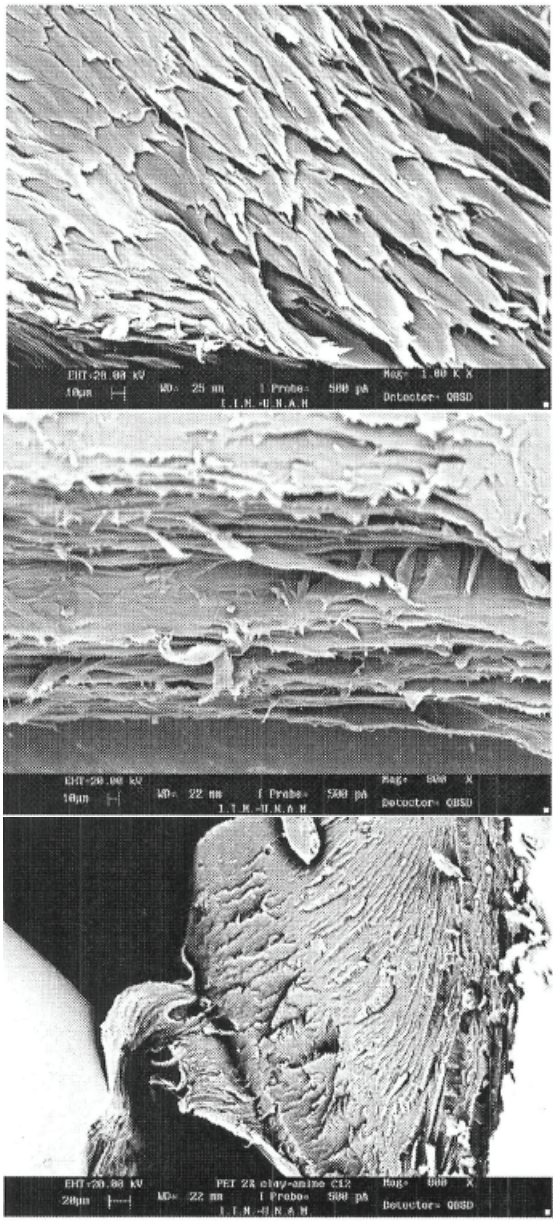

Fig. 2. Micrographs showing the center strained region of tensile test specimens (a) pet, (b) PET+1% Dodecylammonium modified clay, (c) PET+2% Dodecylammonium modified clay

SEM was also used to explore the surface of a PET-PEN-MMT nanocomposite filament obtained by using a capillary rheometer with a die L/D = 20 (at 270 ^{o} C, 10 s^{-1}). A flexible peel of low molecular weight polymer was observed in the section of the filament exposed

to the wall die. Evidence of an internal slip layer is also observed. This may be the cause of the decrease in the shear viscosity observed when clay is added; this effect will be further discussed in the rheology section. This peel was not observed in the system with no added clay (See figure 3). An internal slip layer was also observed. [Calderas et al. 2009]

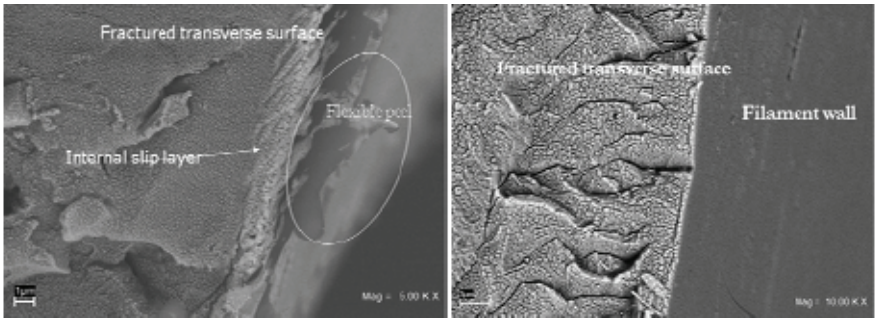

Fig. 3. SEM micrographs of the edge of the capillary filament. Left: PET-PEN blend. Right: PET-PEN blend with 1% clay.

6. Rheology

6.1 Theory

6.1.1 BMP constitutive equation

In this section, we discuss the predicting capabilities of constitutive equations to describe the rheological behavior of nanocomposite systems. Underlying mechanisms are the structural modification under flow and induction or formation of structures. An example of a constitutive equation which describes these processes is the BMP equation of state. This equation [Bautista et al. 1999; Manero et al. 2002] is written here in terms of a stress superposition according to:

$$\underline{\underline{\sigma}} = \sum_{i=1}^{N} \underline{\underline{\sigma}}_i \tag{5}$$

$$\underline{\underline{\sigma}}_i + \frac{\eta_{0i}}{G_{0i}} \xi_i\left(\mathrm{II}_{\underline{\underline{D}}}\right) \overset{\nabla}{\underline{\underline{\sigma}}}_i = 2\eta_{0i}\xi_i\left(\mathrm{II}_{\underline{\underline{D}}}\right)\underline{\underline{D}} \tag{6}$$

$$\frac{d}{dt} Ln\xi_i\left(\mathrm{II}_{\underline{\underline{D}}}\right)^{\lambda_i} = 1 - \xi_i\left(\mathrm{II}_{\underline{\underline{D}}}\right) + \beta_i\left(1 - \mathrm{B}_i\xi_i\left(\mathrm{II}_{\underline{\underline{D}}}\right)\right)\underline{\underline{\sigma}}_i : \underline{\underline{D}} \tag{7}$$

$$\xi_i\left(\mathrm{II}_{\underline{\underline{D}}}\right) = \frac{\eta_i\left(\mathrm{II}_{\underline{\underline{D}}}\right)}{\eta_{0i}}; \qquad \beta_i = k_i\lambda_i; \quad \mathrm{B}_i = \eta_{0i}/\eta_{\infty i} \tag{8}$$

Where $\underline{\underline{\sigma}}_i$ and $\underline{\underline{D}}_i$ the stress and rate of deformation tensors, respectively; $\overset{\nabla}{\underline{\underline{\sigma}}}_i$ denotes the upper-convected derivative of the stress tensor; and λ_i, G_{0i}, η_i, η_{0i} stand for variable relaxation time, elastic modulus, viscosity function and viscosity to low shear rate respectively. $\xi_i\left(\mathrm{II}_{\underline{\underline{D}}}\right)$ are scalars that reflect changes in viscosity due to changes in the structure induced by flow. $\beta_i = k_i\lambda_i$ can be interpreted as an inverse of the energy associated to

the kinetics and structural mechanisms. The two characteristic times λ_{0i} , $\lambda_{\infty i}$ are Maxwell relaxation times to low and high shear rate respectively.

For a mono modal model $(i=1)$, the BMP [Bautista et al. 1999, 2002; Soltero 1999, Manero et al. 2002, 2007; Escalante et al. 2007; Calderas et al. 2009; Herrera et al. 2009, 2010] model is defined by the following equations:

$$\underline{\underline{\sigma}} + \frac{\eta\left(\mathrm{II}_{\underline{\underline{D}}}\right)}{G_0}\overset{\nabla}{\underline{\underline{\sigma}}} = 2\eta\left(\mathrm{II}_{\underline{\underline{D}}}\right)\underline{\underline{D}} \tag{9}$$

$$\frac{d}{dt}Ln\eta\left(\mathrm{II}_{\underline{\underline{D}}}\right)^{\lambda} = 1 - \frac{\eta\left(\mathrm{II}_{\underline{\underline{D}}}\right)}{\eta_0} + k\lambda\left(1 - \frac{\eta\left(\mathrm{II}_{\underline{\underline{D}}}\right)}{\eta_\infty}\right)\underline{\underline{\sigma}} : \underline{\underline{D}} \tag{10}$$

When the viscosity function $\eta\left(\mathrm{II}_{\underline{\underline{D}}}\right)$ tends to a constant, i.e., $\eta\left(\mathrm{II}_{\underline{\underline{D}}}\right) \to \eta_0 = \eta_\infty$. And the codeformational Maxwell derivative is linearized $\overset{\nabla}{\underline{\underline{\sigma}}} \to \partial_t \underline{\underline{\sigma}}$, the BMP reduce to the Maxwell model as a particular case (viscoelastic regime).

6.1.2 Steady state of the BMP model

In the following, we consider the steady-state version of equations (9) and (10), namely.

$$\left(\frac{1 + k\lambda\left(\frac{\eta_0}{\eta_\infty}\right)\underline{\underline{\sigma}} : \underline{\underline{D}}}{1 + k\lambda\underline{\underline{\sigma}} : \underline{\underline{D}}}\right)\underline{\underline{\sigma}} + \frac{\eta_0}{G_0}\overset{\nabla}{\underline{\underline{\sigma}}} = 2\eta_0\underline{\underline{D}}; \tag{11}$$

where the time derivative of the stress are set to zero in Eq. (9), i.e., $\partial_t \underline{\underline{\sigma}} = \underline{\underline{0}}$. The left hand of equation is a structural parameter, which may be considered as a measure of flow-induced departures of structure from a reference state. Here, the reference state is defined as the viscosity at vanishing shear rate η_0 . Equation (11) contains four property materials: (i) two viscosities to low and high shear rate η_0 , η_∞ , (ii) relaxation structural time λ , (iii) elastic modulus G_0 and one fitting numerical parameter k that can be interpreted physically as a kinetic constant for the structure break-down. It is important to note that equation (11) is quadratic in the stress and embodies particular cases discussed elsewhere. [Bautista et al. 1999, Manero et al. 2002].

The BMP model was selected for this study due to its capacity of predicting the thixotropic behavior of structured fluids such as: (i) worm-like micellar solutions, (ii) dispersions of lamellar liquid crystals, (iii) associative polymers, (iv) bentonite suspensions, (vi) polymer like micellar solutions and (vii) nanocomposites. In addition, the model reproducing the complete flow curve for a shear thinning and shear-thickening fluid, i.e. a Newtonian plateau at low and high shear rates, an intermediate power- law region and non-vanishing normal- stress differences; it also gives a reasonable description of the elogational and complex viscosity with finite asymptotic value and mono-exponential relaxation stress relaxation and start-up curves, thixotropy and shear banding flow [Soltero et al. 1999;.Bautista et al. 1999; 2000; 2002, Manero et al. 2002, Escalante et al. 2003, Escalante et al. 2007; Calderas et al. 2009].

Analytical solutions for the simple shear flow are obtained by using this model due to its simplicity as compared to more complex models [Acierno et al. 1976; De Kee et al. 1994; Giesekus 1966, 1982, 1984, 1985, Quemada et al. 2003]. Furthermore, all five parameter of the model are related to the fluid properties and can be estimated from rheological experiments in steady and unsteady state as described elsewhere [Bautista et al. 1999]. The viscosities η_0 and η_∞ can be obtained from low and high-shear-rate plateau in steady shear measurements. G_0 can be obtained by oscillatory shear measurements or from instantaneous stress relaxation experiments. The agreement between the values of G_0 obtained from these two experiments is within 10%[Soltero et al. 1996]. The structural relaxation time λ can be estimated from the intercept of the stress relaxation times at long times alter cessation of steady shear flow, where the intercept is given by $Exp[-G_0\lambda\left(\eta_{ss}^{-1}-\eta_0^{-1}\right)]$, being η_{ss}^{-1} the steady state fluidity (inverse of the viscosity) prior to the cessation of shear flow. The parameter k, in turn, can be evaluated from the stress growth coefficient η^+ from inception of shear flow experiments [Soltero et al. 1999].

6.2 Lineal viscoelastic regime

6.2.1 Multi-modal Maxwell equation

In the case, when the system has a constant structure, the structure parameter and the dimensionless number goes to the unit, i.e., $\xi\left(\mathrm{II}_{\underline{\underline{D}}}\right)=\mathrm{B}_i\rightarrow 1$ the multimodal version of the BMP (Bautista-Manero-Puig) model reduces to the multimodal version of the codeformational Maxwell equation [Bautista et al. 1999, Manero et al. 2002].

$$\underline{\underline{\sigma}}=\sum_{i=1}^{N}\underline{\underline{\sigma}}_i \tag{11}$$

$$\underline{\underline{\sigma}}_i+\lambda_{0i}\overset{\nabla}{\underline{\underline{\sigma}}}_i=2\lambda_{0i}G_{0i}\underline{\underline{D}} \tag{12}$$

In the lineal viscoelastic regime, equations (11, 12) reduces to the Maxwell model, and the well-known storage and loss modules of the Maxwell Model [Bautista et al. 1999, Manero et al. 2002].

$$G''(\omega)=\sum_{i=1}^{N}G_{0i}\frac{(\omega\lambda_{0i})^2}{1+(\omega_0\lambda_i)^2} \tag{13}$$

$$G'(\omega)=\sum_{i=1}^{N}G_{0i}\frac{\omega\lambda_{0i}}{1+(\omega\lambda_{0i})^2} \tag{14}$$

G_{0i} and λ_{0i}, represent characteristic values of moduli and the corresponding relaxation time, respectively. The parameters G_{0i} and λ_{0i} of each sample were calculated using nonlinear regression data of the corresponding oscillatory flow curves G '(ω) and G'' (ω) [Calderas et al. 2009]

6.3 Rheometry

In this section, results for the nanocomposites PET-PEN/MMT clay studied under steady shear, instantaneous stress relaxation and relaxation after cessation of steady shear flow are reported.

6.3.1 Steady shear flow experiments

6.3.1.1 PET-PEN blend

Rheological measurements have been reported for the pure PET and PEN polymers as well as for PET-PEN blends at 270°C using a TA-Instruments AR 1000-N controlled stress rheometer with parallel plates of 25 mm diameter and 0.75 mm gap [Sánchez-Solís et al. 2005a]. The low shear rate viscosity of PEN is about ten times that of PET, and the shear-thinning region of the former starts at 2 s^{-1} while that of PET begins at higher shear rates (around 20 s^{-1}). Shear viscosities of PET-PEN blends processed at 270°C with 2 min residence time tend to a plateau at low shear rates and shear thinning for shear rates larger than 10 s^{-1}. The low shear- rate viscosity was found to increase in a direct relation to PEN content in the blend at 270°C with 2 min residence time. It is important to mention that the extent of transesterification reaction and %transesterification reached the highest values for these conditions. The effect of the extruder processing temperature on the blend was also reported; temperatures at the extruder exit die of 270, 280 and 290°C were applied. Agreement between first Newtonian viscosity and %transesterification was found for the conditions studied.

6.3.1.2 PET-MMT nanocomposite

With respect to PET-MMT nanocomposites, viscosity at low shear rate using the same rheometer have been measured [Sánchez-Solís et al. 2003]. All measures were reported at 270 °C with samples having the same thermomechanical history. The effect of clay content and additives (MAH and PENTA) was studied. It was found that the low shear viscosity (zero shear viscosity) decreased with clay content to values less than half those of PET for 2% clay content. Additives were found to reduce viscosity at 2% clay content even more, but they show no effect at lower clay contents. The effect of diminishing viscosity with clay content (in the 1-2% range) is an important issue to consider. Cost reduction due to the energy savings to process the nanocomposite and better filling of the mold cavities, etc., are some benefits. However, the effect is far from being totally understood, but from what has been discussed in this chapter so far, the difference in nanoparticle concentration in the surface as compared to the bulk nanocomposite (see section 2), as well as the formation of a slip layer (see section 5) may be the key issues to explain this effect.

To address the effect of clay modified with different additives (MAH, PENTA and the alkylammonium chlorides, see section 4.2 for details) [Sánchez-Solís et al. 2004] three different PET samples were studied: pellets of PET as received, PET extrudedonce, and PET extruded and mold-injected. It was shown that while the decrease in the viscosity due to extrusion is relatively small (from 400 to 300 Pa s). The large drop observed in molded samples is quite drastic (from 300 to 30- 40 Pa s). This extremely large decreasein the shear viscosity of the molded samples is also accompanied with a strong decrease in the viscousmodulus of almost a decade as measured in linear viscoelastic oscillatory tests (as will be discussed in the oscillatory flow section). Again it was demonstrated that the shear

viscosity of the PET-MMT nanocomposites decreased with clay content (up to 2%) as compared to PET extruded once. Newtonian plateau was found to extent to higher shear rates (onset of shear thinning) with clay content (no additives). Nanocomposites with additives (MAH and PENTA) showed similar trends in viscosity as compared to systems with no additives, which lead to the conclusions that the main effect in viscosity changes was attributable to the nanoparticles alone. The rheological properties for the 1% and 2% clay (nDodecylammonium) systems were also reported. Molecular weight was found to diminish with the addition of modified clay (nDodecylammonium) and while the viscosity of the 1% modified clay (exfoliated) system showed a similar viscosity curve as extruded PET (constant viscosity in almost all the shear rate range studied) but with lower viscosity values, the 2% modified clay system (non exfoliated) exhibits a loss of Newtonian plateau and lower values of viscosity throughout the range studied.

6.3.1.3 PET-PEN-MMT nanocomposite

As expected from previous results, a decrease in the shear viscosity upon clay addition was found in the PET-PEN–MMT clay nanocomposites [Sánchez-Solís et al. 2005b]. The clay–Na+ blend presented a slightly larger zero shear viscosity than the other blends (clay-MAH and clay-C18), but the onset for shear-thinning is similar to that of the precursor polymers PEN and PET.

The steady-state shear viscosity for the pure PET-PEN polymer matrix has been compared to that of a PET 80%- PEN 20% - 1% MMT organically modified clay nanocomposite (quaternarium ammonium salt modified clay), after processing the matrix at the same conditions used to process the nanocomposites. For this clay nanocomposite the zero shear viscosity is lower than that of the unfilled matrix [Calderas et al. 2009]. This behavior is in agreement with that of the previous discussion.

6.3.2 Oscillatory flow

6.3.2.1 PET-PEN blend

For the PET-PEN blend, a high degree of correlation between the storage modulus, G′ (as measured in linear viscoelastic regime), the % transesterification and the steady state shear viscosity was found. To study compatibility between PET and PEN polymers, master curves of G′ versus G′′ were prepared. A good correlation was found at the three temperatures (270, 280 and 290 °C) and two extruder residence times (2 and 4 min) except in the low frequency region. Slopes lower than two in the low frequency region of the elastic modulus were associated to the presence of an elastic network.

These results suggest that the same degree of compatibility is found at all processing conditions studied and this was verified with Tg measurements, revealing only one Tg for all blends.

6.3.2.2 PET-MMT nanocomposite

Complex viscosity (measured in the linear viscoelastic region) was found to decrease with clay content in a similar fashion as steady state shear viscosity (as mentioned in section 6.3.1.2) for PET-MMT nanocomposites. However, decreasing viscosity with frequency was not observed as opposed to the shear viscosity. This result leads to the conclusion that continuous shear caused particle flow alignment with the consequent shear thinning

behavior. Storage modulus (G′) was measured, and a decrease of viscoelastic properties with clay addition was observed, in agreement with continuous shear viscosity. The presence of nanoparticles was evidenced in the low frequency region with a G′ slope change (deviation from the Maxwell slope value of 2). This is an evidence of solid-like behavior (frequency independent G′) in these systems.
As was previously mentioned (section 6.3.1.2) a large decrease in viscosity and storage modulus G′ was observed for pure PET when the sample was mold-injected. This is directly related to a molecular weight loss (measured and reported). Storage modulus was found to increase in the exfoliated samples surpassing the G′ values of extruded PET. This effect was shown to be independent of molecular weight changes and was attributed to the nanoparticles only. In the nanocomposites, the values of the G´ showed no direct relation to sample molecular weight, i.e., one non-exfoliated sample with one of the lowest molecular weight reached G′ values higher than those of extruded PET, which was attributed to a high degree of particle dispersion in the PET matrix.

6.3.2.3 PET-PEN-MMT nanocomposite

For the PET-PEN-MMT nanocomposite, a solid-like response was reported for the unmodified clay (clay-Na^+) and Octadecylammonium modified clay (clay-C18) [Sánchez-Solís et al. 2005b]. Such behavior was ascribed to larger particle–polymer interactions, which lead to a larger number of molecular entanglements in the blend.
This strong polymer-nanoparticle interaction was studied in a PET-PEN-organically modified MMT in detail by performing instantaneous stress relaxation, relaxation after cessation of flow and start-up rheological test [Calderas et al. 2009]. Results are discussed in the following sections.

6.3.3 Instantaneous stress relaxation

In this test, an initial small-amplitude strain is applied to the sample during a period t1 (which depends on the apparatus used). This period in the present case is 0.06 s. Then, for all t > t1, the stress is allowed to relax. The stress relaxation modulus G(t), i.e., the shear stress divided by the applied strain, is plotted versus time. The stress was monitored until a terminal slope was reached. The time necessary to reach the terminal slope was found to be about 60 s for all materials. All systems showed two main modes of relaxation times (λ), a slow mode associated to the initial slope (short times) and a fast one associated to the final slope (longer times).
As expected, pure PEN (largest steady shear viscosity) possesses the highest initial modulus (around 600 Pa), but the transition between the two main modes of relaxation is smoother as compared to the other systems. The sharpest shift between the two main modes is observed to occur in pure PET, while for the PET-PET blend and for the nanocomposite, the shift is not as sharp as for pure PET, nor as smooth as for pure PEN.
Normalized relaxation curves (with initial G(t) value) for three systems were analyzed in a log-log plot. PET showed a rapid and more pronounced initial relaxation, while in the other systems (PET-PEN and PET-PEN-clay) the presence of PEN and the clay somehow restricts the rapid relaxation and there is a rapid change towards the slow mode which is evidenced by an earlier change of slope. The response at long times for the instantaneous stress relaxation curve has been associated to the polymer-filler interactions. For these systems the

terminal slope is similar for the pure PEN and for the nanocomposites system. In the case of the polymer blend, PET and PEN chains form a network promoted by the trans-esterification reaction that occurs at the processing conditions, which produces a copolymer and mutual crosslinking. For the nanocomposites, the relaxation is also restricted but the presence of the clay induces different dynamics. In this case, the relaxation is not as slow as for the polymer blend, (this is clearly observed in the large slope at long times) possibly caused by a particular polymer-clay interactions, since the high molecular weight chains are absorbed preferentially in the clay galleries, thus allowing more mobility in the non-absorbed low-molecular weight chains. In addition, it has been reported that in the presence of the clay in the polymer matrix somehow restricts the amount of cross-linking and thus the copolymer formation (see discussion at the end of section 1).
A Fourier Transform (FT) frequency response was obtained from the relaxation curves and compared to the linear oscillatory data. A good agreement was found between both viscoelastic data.
The results were modeled by the above exposed rheological equation of state [see section 6.1]. The model was used to find the characteristic times of the slow and fast modes for the systems. The model for pure PEN requires 3 relaxations times or modes, pure PET and the PET-PEN blend require 4 relaxation times and the nanocomposites requires 5 modes, revealing the complexity added by the presence of the clay. The two main modes for the systems are disclosed in Table 3. Comparatively, the characteristic time of the slow mode in the PET-PEN systems is the largest, reflected in the plateau of the relaxation curve and related to the effect induced by the transesterification reaction occurring in the system which produces an amount of cross-linking [Calderas et al. 2009]. The characteristic times of the fast modes have similar values.

6.3.4 Start-up of shear flow

Stress growth was reported as a function of time showing that the material with added clay reaches the maximum stress. This maximum value reflects the initial elasticity of the system, evidencing the formation of an elastic network induced by strong polymer-matrix interactions in the nanocomposite. Curves for PET and PET-PEN blend overlap, showing no significant change. The amplitude of the overshoots has been proposed to be related to the degree of exfoliation of the nanoclays. Furthermore, overshoots in polymer-clay systems have been attributed to the break-down of a clay platelet network [Calderas et al. 2009].

6.3.5 Relaxation after cessation of steady state flow

In this experiment, the sample is sheared at constant and steady shear rate (10 s^{-1}). At time t = 0, the flow is suddenly stopped and the relaxation of the stress is followed as a function of time. PET was reported to show a fast relaxation, while PET-PEN and PET-PEN-MMT display a similar slope at long times. The behavior at long times reflects chain cross-linking in the case of PET-PEN blend and a polymer-clay interactions in the case of the nanocomposites.
Table 4 shows the values of the two main relaxation times for the samples. With exception of PEN, all curves display similar initial fast relaxation time. At long times, PET shows a fast decay to very slow value of stress, i.e., below the rheometer resolution. The relaxation curve for the PET-PEN system seems to stabilize at long times and presents the largest

characteristic times of the slow mode (see Table 4). This may be attributed again to the cross-linking induced by the reaction among the polymers, while the PET-PEN-clay blend shows a small relaxation time of the slow mode. This system is thought to have experienced a structural break up due to the constant shear flow imposed before the relaxation dynamics and thus the system becomes less structured (possibly flow alignment of clay nanoparticles) affecting the relaxation dynamics after flow cessation.

Modes	*PEN*	*PET*	*PET-PEN*	*PET-PEN/MMT*
Slow	6.83	11.95	13.82	6.50
Fast	0.12	0.10	0.13	0.09

Table 3. Main Relation times $\lambda[s]$ for the materials as obtained from instantaneous stress relaxation data

Modes	*PEN*	*PET*	*PET-PEN*	*PET-PEN/MMT*
Slow	1.24	0.312	1.74	1.50
Fast	0.10	0.017	0.016	0.016

Table 4. Main relaxation time $\lambda[s]$ obtained from stress relaxation after cessation of steady shear

7. Conclusions

A comprehensive review on the preparation by melt extrusion and characterization of PET-MMT and PET-PEN-MMT nanocomposites was presented. Emphasis was made in presenting results related to the mechanical properties, morphology and flow characteristics of nanocomposites using different experimental techniques. The influence of several factors such as processing conditions, clay modification, clay content, %transesterification and compatibilizing additives was discussed and analyzed. Several important issues arise from the analysis of these systems, i.e. there is a decrease in shear viscosity with clay addition which still is far from being totally understood. However this effect can be beneficial to processing, reducing energy necessary to melt compounding and injecting and filling mold cavities. Nevertheless, special care has to be taken in order to reduce sample sagging during processing due to small viscosity, and hence temperature profiles will have to be adjusted accordingly. The formation of a slip layer in the surface of flowing samples and the migration of nanoparticles away from the surface seem to be key issues to explain the viscosity reduction effect, even though other factors such as slippage at particle-polymer interphase, particle alignment, particle migration and polymer absorption in the particles will have to be studied to fully understand this effect. Solid-like behavior is another important effect and it seems to be strongly associated to polymer-particle interaction. Final, it still not clear if clay exfoliation, clay modification or clay addition are sufficient conditions to obtain high performance nanocomposites and further investigation will be required to understand and finally produce adequate nanocomposites for specific applications.

8. References

Alexandrova, L., Cabrera, A., Hernández, M.A., Cruz, M.J, Abadie, M.J.M., Manero, O., Likhatchev, D.,(2000). Mechanism and kinetics of transesterification in

poly(ethylene terephthalate) and poly(ethylene terephthalate) and poly (ethylene 2,6-naphtalene dicarboxylate) polymer blends. Polymer, 43, 5397-5403, ISSN: 0032-3861

Bautista, F., De Santos J.M., Puig, J.E., Manero, O. (1999), Understanding thixotropic and antithixotropic behavior of viscoelastic micellar solutions and liquid crystalline dispersions. I. The model. *J Non-Newtonian Fluid Mech*, 80, 93-113, ISSN: 0377-0257.

Bautista, F., Soltero, F.F.A, Pérez–López, J.H., Puig, J. E., Manero, O. (2000). On the shear banding flow of elongated micellar solutions, *J Non-Newtonian Fluid Mech*, 94, 57-66, ISSN: 0377-0257.

Bautista, F., Soltero, J.F.A., Macias, E.R., Puig, J. E., Manero, O. (2002). Irreversible thermodynamics approach and modeling of shear-banding flow of wormlike micelles.J. *Phys Chem B*, 106, 50, 13018-13026, ISSN: 1520-6106.

Bautista, F., Pérez-López, J.H., García J.P., Puig J.E. Manero, O. (2007). Stability analysis of shear banding flow with the BMP model.*J Non-Newtonian Fluid Mech,* 144, 160-169, ISSN: 0377-0257.

Bautista, F., Muñoz, M., Castillo-Tejas, J., Perez-Lopez, J.H., Puig, J.E., Manero, O. (2009). Critical phenomena analysis of shear-banding flow in polymer-like micellar solutions. 1. Theoretical approach, *J Phys Chem Part B*, 113, 50, 16101-16109, ISSN: 1520-6106.

Calderas, F., Sánchez-Solis, A., Maciel, A., Manero, O. (2009). The Transient flow of the PETPEN-Montmorillonite clay Nanocomposite. *Macromol Symp*, 283-284, 354-360, ISSN: 1022-1360.

Chen P, Music K and McNeely G, Transesterified PET/PENviamelt extrusion. WO Patent WO 96/35571 (1996).

Collins, S., Kenwright, A. M., Pawson, C., Peace, S. K., Richards, R. W., MacDonald, W. A., Mills, P. (2000). Transesterification in Mixtures of Poly(ethylene terephthalate) and Poly(ethylene naphthalene-2,6-dicarboxylate): An NMR Study of Kinetics and End Group Effects.*Macromolecules*, 33, 8, 2974-2980, ISSN: 0024-9297.

De Andrade Lima, L.R.P., Rey A.D. (2006), Pulsatile flows of Leslie-Ericksen liquid crystals. *J Non-Newtonian Fluid Mech,* 135, 32-45, ISSN: 0377-0257.

De Andrade Lima, L.R.P., Rey, A.D. (2006). Back-Flow in Pulsatile Flows of Leslie Ericksen Liquid Crystals, *Liquid Crystals*, 33, 6, 711-712, ISSN: 0267-8292.

DeKee, D., Chan Man Fong, C.F. (1994). Rheological Properties of Structured Fluids, *Polym Eng Sci*, 34, 5, 438-445, ISSN: 0032-3888.

Devaux, J., Godard, P., Mercier, J.P. (1982). Bisphenol-A polycarbonate-poly(butylenes terephthalate) transesterification. II. Structure analysis of the reaction produces by IR and ^{1}H and ^{13}C NMR. *J Polym Sci Part B: Polym Phys*, 20, 10, 1881-1894, ISSN: 0887-6266.

Escalante, J.I., Macias, E.R., Bautista, F., Pérez-López, J.H.,Soltero, J.F.A., Puig J.E., Manero, O. (2003). Shear-banded flow and transient Rheology of cationic wormlike Micellar solutions.*Langmuir,* 19, 17, 6620-6626, ISSN: 0743-7463.

Escalante, J.I., Escobar, D. M., E.R., Perez-Lopez, J.H., Bautista, F., Mendizabal, E., Puig, J.E., Manero, O. (2007). Effect of a hydrotope on the viscoelastic properties of polymer-like micellar solutions. *Rheol Acta*, 46., 685-691, ISSN: 0035-4511.

Giesekus, H. (1982). A Simple Constitutive Equation for Polymer Fluids Based on the Concept of Deformation-dependent Tensorial Mobility, J Non-Newtonian Fluid Mech, 11, 69-109, ISSN: 0377-0257.

Giesekus, H. (1984). On Configuration-Dependent Generalized Oldroyd Derivatives, *J Non-Newtonian Fluid Mech*, 14, 47-65, ISSN: 0377-0257.

Giesekus, H. (1985). Constitutive equation for Polymer Fluids Based on the Concept of Configuration dependent Molecular Mobility: A Generalized Mean-Configuration Model. *J Non-Newtonian Fluid Mech*, 17, 13, 349-372, ISSN: 0377-0257

Godard, P., Dekoninck, J.M., Devlesaver, V., Devaux, J. (1986). *J. Polym. Sci. Part A: Polym. Chem*, Molten bisphenol-A polycarbonate-polyethylene terephthalate blends. II. Kinetics of exchange reaction, 24, 12, 3315-3324, ISSN: 0887-624X.

Herrera, E.E., Calderas, F., Chávez, AE., Manero, O., Mena, B. (2009), Effect of random longitudinal vibrations pipe on the Poiseuille flow of a complex liquid, *Rheol Acta*, 48, 7, 779-800, ISSN: 0035-4511.

Herrera, E.E., Calderas F., Chávez, A.E., Manero, O. (2010). Study on the pulsating flow of a worm-like micelar solution. *J Non-Newtonian Fluid Mech,* 165, 174-183, ISSN: 0377-0257.

Kenwright, A.M., Peace, S.K., Richards, R.W., Bunn. A., MacDonald, W.A. (1999), Transesterification in poly(ethylene terephthalate) and poly(ethylene) naphthalene 2,6-dicarboxylate) blends; the influence of hydroxyl end groups, *Polymer*, 40, 21, 5851-5856, ISSN: 0032-3861.

Lee, H.M., Suh D.J., Kil, S.B., Park, O.O., Yoon, K.H., Rheological anomalies of the poly(ethylene 2, 6-naphthalate) and polyethylene terephthalate) blends depending on the compositions, Korea–*Australy Rheol* J, 11, 3, (1999), 219-223, ISSN: 1226-119X

Manero, O., Bautista, F., Soltero, J.F.A., Puig, J.E. (2002). Dynamics of worm-like micelles: the Cox-Merz rule. *J Non-Newtonian Fluid Mech*, 106, 1, 1-15, ISSN: 0377-0257.

Manero, O., Pérez-López, J.H., Escalante, J.I.,Puig, J.E., Bautista, F. (2007), A thermodynamic approach of rheology of complex fluids: The generalized BMP model. *J. Non-Newtonian fluid Mech,* 146, 1-3, 22-29, ISSN: 0377-0257.

Okamoto, M. (2006). Recent advances in polymer/layered silicate nanocomposites: an overview from science to technology.*Mat Sci Tech*, 22, 7, 756-779, ISSN: 0267-0836.

Medina, R. M., Likhatchev, D., Alexandrova, L., Sánchez-Solís, A., Manero, O. (2000). Mechanism and kinetics of transesterification in poly(ethylene terephthalate) and poly(ethylene 2,6-naphthalene dicarboxilate) polymer blends. *Polymer*, 45, 8517–8522, ISSN: 0032-3861.

Milan, K., Martin, S., Jana, M., Jana K., Antonín, S., Ralf, T., Chirtian, F. (2007). Recycled PET-Organoclay nanocomposites with enhance processing properties and thermal stability. *J App Polym Sci,* 106, 2092-2100, ISSN: 0021-8995.

Sánchez–Solis, A., Garcia–Rejón, A., Martínez-Richa, A., Calderas, F., Manero, O. (2005a). Properties of pet-pen blends produced by extrusión and injection blow-molding.*J Polym Eng,*25, 6, 553-570, ISSN: 0334-6447.

Sanchez-Solis, A., Garcia-Rejón, A., Mirna Estrada, R., Martinez-Richa, A., Sanchez, G., Manero, O. (2005b). Properties of poly(ethylene terephthalate)-poly(ethylene naphthalene 2,6-dicarboxylate) blends with montmorillonite clay. *Polym Int*, 54, 1669–1672, ISSN: 0959-8103.

Sánchez-Solís, A. Romero-Ibarra I. Estrada M. R., Calderas F and Manero, O. (2004). Mechanical and rheological studies on polyethylene terephthalate-montmorillonitenanocomposites. *Polym Eng Sci* 44, 6, 1094-1102, ISSN: 0032-3888.

Sánchez–Solis, A., Garcia–Rejón, A., Manero, O. (2003). Production of nanocomposites of PET-montmorillonite clay by an extrusion process. *Macromol Symp, 192*, *281-292,* ISSN: 1022-1360.

Sanchez-Solis, A., Estrada, M.R., Cruz, J., Manero, O. (2000). On the properties and processing of polyethylene terephthalate/styrene-butadiene rubber blend. *Polym Eng Sci,* 40, 5, 1216-1225, ISSN: 0032-3888.

Suel, E. V., Anne C. Chinellato, Guo-Hua Hu, Luiz A. Pessan. (2007). Preparation of Polymer(ethylene terephthalate)/Organoclaynanocomposites using a Polyester ionomer as compatibilizer. *J Polym Sci: Part B: Polym Phys*, 45, 3084-3091, ISSN: 0887-6266.

Suprakas, S. R. and Okamoto, M. (2003). Polymer/layered silicate nanocomposites: a review from preparation to processing, *Prog Polym Sci,* 28, 1539–1641, ISSN: 0079-6700.

Y. Ke, C. Long, Z. Qi., (1999)., Crystallization, properties, and crystal and nanoscale morphology of PET-clay nanocomposites, *J Appl Polym Sci*, 71, 1139-1146, ISSN: 0021-8995